Nucleic Acids Research, 1993, Vol. 21, No. 3 561–568

$B_I - B_{II}$ transitions in B-DNA

Brigitte Hartmann, Daniel Piazzola and Richard Lavery*
Laboratoire de Biochimie Théorique, CNRS URA77, Institut de Biologie Physico-Chimique, 13 rue Pierre et Marie Curie, Paris 75005, France

Received October 16, 1992; Revised and Accepted December 23, 1992

ABSTRACT

Molecular modelling is used to study the conformational and energetic aspects of $B_I - B_{II}$ transitions within the backbone of a B-DNA dodecamer d(CATGACGTCATG) whose fine structure has previously been determined by molecular modelling combined with NMR spectroscopy. It is shown that while the dodecamer under investigation does not contain any B_{II} junctions, the central CpG step can most easily undergo the transition. More generally, it is also found that the base sequence and hence the backbone geometry of a DNA segment, strongly influences both the conformational impact of the transition, the associated energy barrier and the stability of the resulting B_{II} state.

INTRODUCTION

Single crystal X-ray analysis of DNA oligomers has brought to light a wealth of structural detail within the double helix. Sequence effects are now known to include a wide variety of conformational changes, concerning both mutual base positions and modifications of the phosphodiester backbones. In many cases however there is, as yet, no clear understanding of the energetics of such deformations or of the mechanisms of associated structural transitions.

One particularly interesting case involves the so-called B_I and B_{II} conformations which have been observed crystallographically within B-DNA oligomers (1,2). These conformations influence the position of the phosphate group with respect to the grooves of the double helix. The more common B_I state places the phosphate in a roughly symmetric position with respect to both grooves, while the B_{II} state swings the phosphate around towards the minor groove. This transition involves coupled changes of two dihedral angles ϵ (C4′-C3′-O3′-P) and ζ (C3′-O3′-P-O5′) which pass from (t,g−) in B_I to (g−,t) in B_{II}. The conformation of the phosphate within a given dinucleotide junction can thus be characterized by the difference $\epsilon - \zeta$ which passes from roughly −90° in B_I to roughly +90° in B_{II} .

Whether the less common B_{II} state actually exists in solution is not clear and it has been suggested that its appearance may be linked to crystal packing effects (3–5). Unfortunately solution studies involving NMR spectroscopy are hindered by the fact that neither ϵ nor ζ can be determined unambiguously. Heteronuclear ^{31}P-^{1}H COSY spectroscopy gives access to the H3′-C3′-O3′-P coupling constant which, with the help of a modified Karplus curve (6), can be linked to the ϵ dihedral. For typical coupling constants, this curve (figure 1) however yields two conformationally feasible values which can generally correspond to either B_I or B_{II} states. Although the value corresponding to a B_I conformation is generally chosen, more data is actually required to eliminate the second possibility.

An alternative route to determining the $B_I - B_{II}$ state involves the chemical shift of the phosphorus atoms within an oligomer. It has also been proposed that low field signals correspond to B_{II} conformations, or to equilibria in which B_{II} conformations make a substantial contribution (7,8). In one case, involving a GA mismatch, this technique, combined with a molecular dynamics simulation (9), has been used to justify the presence of a B_{II} conformation at the level of the mismatch, a conclusion also supported by crystallographic studies (10).

In an attempt to clarify the conformational and energetic aspects of $B_I - B_{II}$ transitions within DNA oligomers we have undertaken a systematic modelling study using the JUMNA program (11) which is specifically designed for modelling nucleic acids. We have chosen to study a biologically relevant DNA sequence, the dodecamer CATGACGTCATG whose central hexamer corresponds to the CRE (cyclic AMP responsive element) binding site (12–13). We have recently been able to present a detailed fine structure for this oligomer based on JUMNA energy minimisation combined with extensive NMR NOESY and COSY data (14). This dodecamer is a good example for study, firstly, because an excellent agreement with the NMR data gives us confidence in the fine structure that has been proposed. Secondly, this structure shows a number of interesting departures from the canonical B form which may well be involved in its specific recognition. Most notably the ^{31}P data show that the phosphates of 3 dinucleotide junctions (T3pG4, C6pG7, C9pA10) resonate at relatively low field and this could be indicative of B_{II} conformations. In the fine structure proposed we have only found a tendency towards the B_{II} state (with $\epsilon - \zeta$ values of roughly −30° compared to −90° in B_I and +90° in B_{II}). In the present study we go beyond this result by making controlled $B_I - B_{II}$ transitions involving most of the dinucleotide junctions of the dodecamer and discussing both the energetic and conformational aspects of such transitions. This data enables us

* To whom correspondence should be addressed

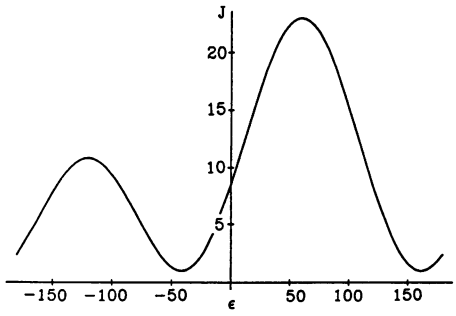

Figure 1. Modified Karplus curve relating the coupling constant J (Hz) for H3'-P to the dihedral angle ε (C4'-C3'-O3'-P) in degrees.

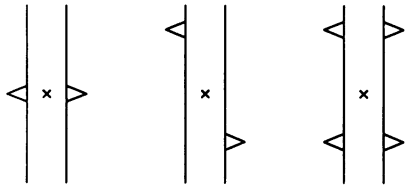

Figure 2. Schematic diagram indicating the symmetry equivalent sites for B_{II} junction conformations within the CRE dodecamer. Each B_{II} site is indicated by a horizontal 'V'. The cross indicates the centre of inversion symmetry of the dodecamer. Left: C6pG7, Centre: C9pA10, right: T3pG4 and C9pA10.

Table 1. B_I-B_{II} transition energetics within the dodecamer CATGACGTCATG (energies in Kcal/mol, reference energy of the dodecamer −593.8 Kcal/mol).

Junction	$E(B_{II})$	$E(B_{II}-B_I)$	Barrier
C6pG7	−591.9	1.9	4.6
T3pG4	−586.7	7.1	7.6
C9pA10	−585.7	8.1	8.6
T3pG4+C9pA10	−597.4	−3.6	15.0
G4pA5	−588.7	5.1	6.4
A5pC6	−590.4	3.4	11.0
G7pT8	−583.8	10.0	15.0
T8pC9	−591.5	2.3	7.6

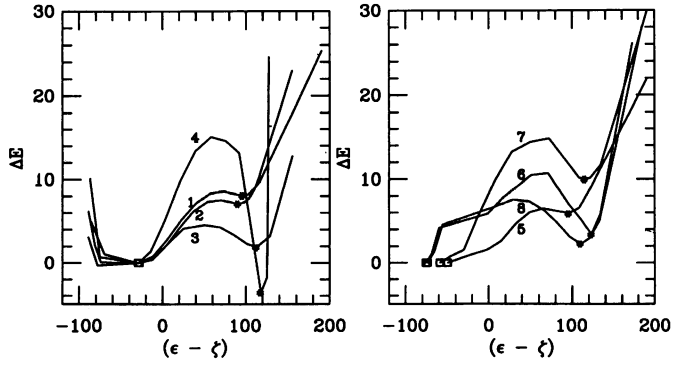

Figure 3. Deformation energy (Kcal/mol) associated with the B_I-B_{II} transitions as a function of $\epsilon-\zeta$ (°). Squares indicate the B_I minima and stars the B_{II} minima. The numbers indicate the junctions involved: (1) T3pG4, (2) C9pA10, (3) C6pG7, (4) T3pG4+C9pA10, (5) G4pA5, (6) A5pC6, (7) G7pT8 and (8) T8pC9.

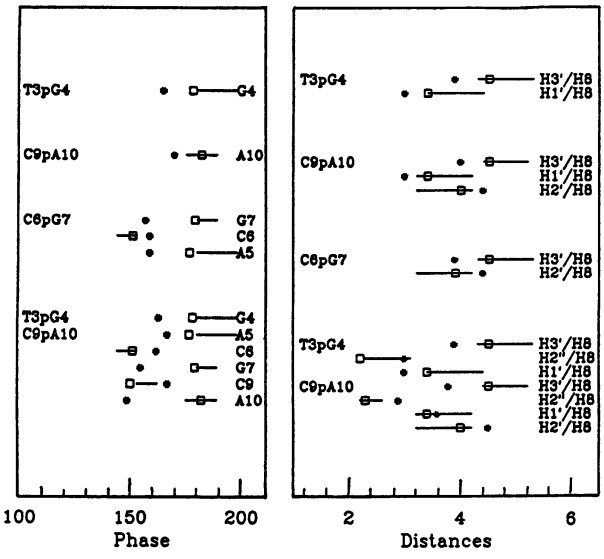

Figure 4. Correspondence between the optimized conformations and the NMR data of the CRE oligomer for steps with phosphates resonating at low field. Only those data changing by more than 5° or 0.2Å are shown. Left: sugar phase angles (°), right: interproton distances (Å). Values coming from B_I model conformations are indicated by squares, while stars show the values after the transition to B_{II} junctions. Horizontal lines indicate the NMR error bars.

to draw clear conclusions concerning the presence of B_{II} conformations within the dodecamer under study and also points to more general rules which influence the probable appearance of such conformations within other sequences.

METHODOLOGY

The JUMNA (Junction Minimisation of Nucleic Acids) program, described in detail in earlier publications (15−19), has already been employed for studying base sequence effects within the various allomorphs of DNA and RNA, the conformation and stability of triple helices, the mechanism of base pair opening and the specificity of DNA-drug interactions. The use of internal coordinates combined with helicoidal parameters which position each nucleotide within a nucleic acid fragment, reduce the number of variables representing the molecule and thus speed up and facilitate conformational searches. This approach also simplifies the introduction of helical symmetry and enables helical deformations to be modelled in a controlled way. The force field used has also been fully documented (20−22). Solvent effects are currently modelled by a simple distance dependent dielectric function of sigmoidal form (21,23) and counterion damping is dealt with by a reduction of total phosphate charges to −0.5e.

This approach seems to be well adapted to modelling DNA oligomers since earlier work has shown many successful correlations with experimental data. In the case of the CRE dodecamer (CATGACGTCATG), unconstrained minimisation with the JUMNA program led to a conformation, termed I(a), almost identical to that obtained with full NMR constraints, termed Ia(C). The two conformations differ only by a slight repuckering of a single sugar (30° change in phase) and were separated by less than 2 Kcal/mol in internal energy.

In the following study the conformation Ia(C) is used as a starting point for the calculations. B_I to B_{II} transitions are induced by imposing chosen values for the ε dihedral of the

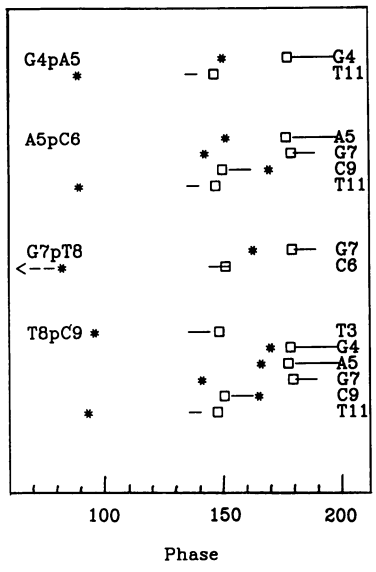

Figure 5. Correspondence between the optimized conformations and the NMR data of the CRE oligomer for steps with phosphates not resonating at low field. See caption to figure (4) for details.

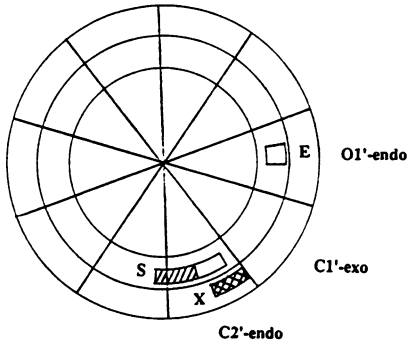

Figure 6. Definition of the pucker states denoted S, X and E on the pseudorotation ring. Sucessively larger circles indicate amplitudes of 30°, 40° and 50°. Open rectangles correspond to pyrimidines, hatched rectangles to purines and cross-hatched rectangles to all nucleotides.

desired dinucleotide junction via harmonic constraints (using a force constant of 200 Kcal/mol/rad^2). In cases where it was necessary to verify if the resulting conformations were compatible with the NMR data on the CRE dodecamer, we also imposed constraints on the phase angles of the deoxyribose rings using harmonic constraints (again with a force constant of 200 Kcal/mol/rad^2) outside the experimentally determined bracket of possible values. NOESY distance constraints were not imposed in these cases since they contribute little towards the determination of the dodecamer conformation once the sugar puckers have been fixed. This finding is discussed in detail in our earlier publication (14).

Note that since the CRE sequence exhibits inversion symmetry, the conformation of the dodecamer would also be expected to respect this symmetry. That this is indeed the case is justified by the NMR data which show that both strands of the duplex are identical. The backbone conformation of the junction C1pA2

Table 2. COSY data for the CRE dodecamer (°). Both of the possible solutions for the e dihedral are indicated.

Residue	Phase	$\epsilon(B_I)$	$\epsilon(B_{II})$
A2	180–188		
T3	135–145		
		−166	−74
G4	180–200		
		−165	−75
A5	180–200		
		−175	−65
C6	145–155		
		−162	−78
G7	180–190		
		−175	−65
T8	145–155		
		−168	−72
C9	153–162		
		−164	−76
A10	175–190		
T11	135–140		

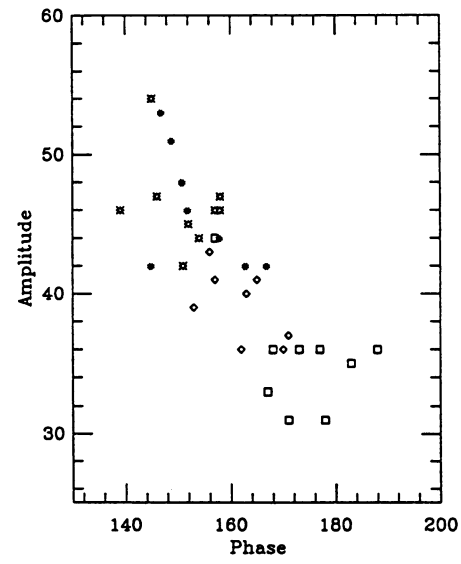

Figure 7. Correlation between sugar phase and amplitude (°) for junctions involving B_{II} phosphate conformations: Model results are indicated by (*) for the 5′-sugar and (◇) for the 3′-sugar, while crystallographic results are indicated by (⊠) for the 5′-sugar and (□) for the 3′-sugar.

in the first strand is thus the same as that of the corresponding junction in the second strand (at the opposite end of the dodecamer). Similarly if any B_I-B_{II} transitions occur within the dodecamer, the resulting conformations must also respect this symmetry. B_{II} states will therefore always occur at two equivalent junctions (one in each strand). In the case of the central C6pG7 junction such a transition will thus lead to two B_{II} phosphates facing one another. For the remaining junctions the transitions will be staggered and result in a B_{II} phosphate facing a B_I phosphate. Both these possibilities are investigated in the following study.

Comparisons with crystallographic data are limited to 5 recent high-resolution decamer structures (5,10,24,25) which due to their crystal space groups are apparently less susceptible to packing effects than earlier dodecamer results. Both these

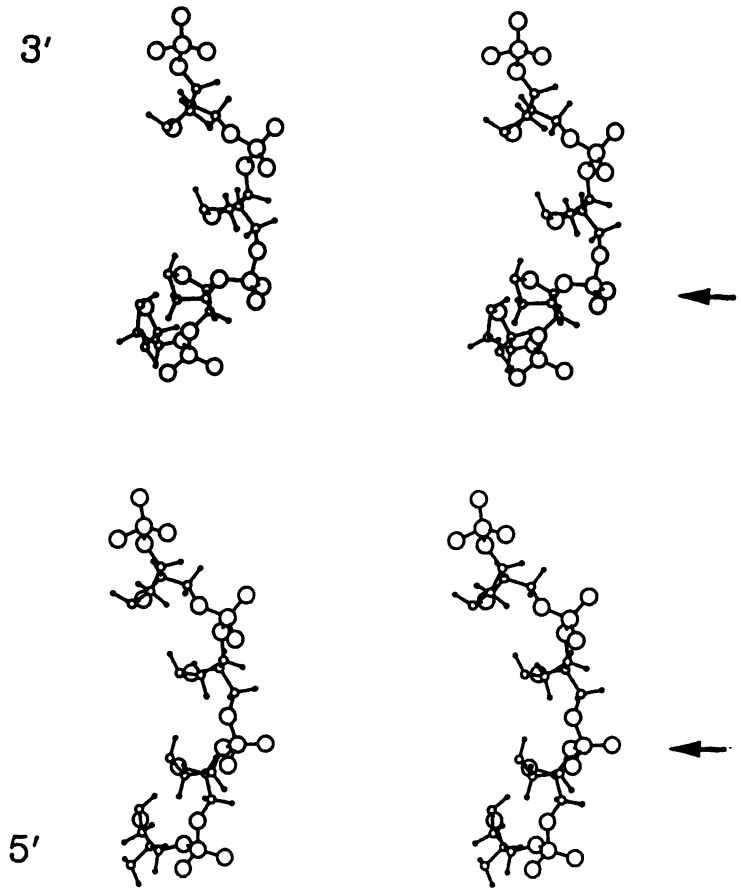

Figure 8. Stereographic diagram showing the B_I (below) to B_{II} (above) conformations of the central phosphate linkage (C6pG7, indicated by an arrow) within a short backbone segment of the CRE oligomer.

experimental conformations and the model conformations obtained with JUMNA are analysed using the CURVES algorithm (26,27) which determines a full independent set of helicoidal parameters related to an optimal curvilinear helical axis. These parameters obey the Cambridge convention for DNA (28). This approach enables fine details of DNA structure, including axis kinking or bending, to be compared in a reliable and quantitative way.

RESULTS AND DISCUSSION

Using the CRE dodecamer as an example we will now look at the energetics and structural aspects of B_I-B_{II} transitions and attempt to answer the question of whether any B_{II} junctions can play a significant role in the solution conformation of this oligomer.

Energetics of the B_I-B_{II} transition

For each dinucleotide junction of the dodecamer studied the starting conformation was that obtained in our earlier work taking into account constraints to NMR data (14). The B_I-B_{II} transition was provoked by fixing the appropriate ϵ dihedral at values varying from roughly 180° to −70°. As this change is made, the adjacent ζ dihedral undergoes coupled changes (g → t) leading to the conformational transition desired. The characteristic measure of $\epsilon-\zeta$ is found to change roughly from −100° to +100°.

The first study concerns the steps whose phosphates resonate at relatively low field, T3pG4, C6pG7 and C9pA10, and which show conformations slightly deformed towards the B_{II} state within the dodecamer conformation. As mentioned above, only the central step C6pG7 will have B_{II} in both strands at the same dinucleotide level (figure 2, left). The other two steps lead to two B_{II} phosphates which do not face one another (figure 2, centre). Due to this difference, we have also considered a coupled transition of T3pG4 and C9pA10 which leads to two dinucleotide steps with B_{II} in both strands (figure 2, right).

The deformation energy curves for these transitions are given in figure 3 (left hand side) as a function of $\epsilon-\zeta$. Minima found after releasing constraints on ϵ are indicated by stars. In all cases the transition is seen to involve an energy barrier at an $\epsilon-\zeta$ value of roughly 70°. We can thus conclude that the $\epsilon-\zeta$ values of roughly −30° observed for these steps in the dodecamer conformation clearly belong to the B_I family. It can also be seen that the B_{II} minima are more sharply defined than the B_I state. In connection with the location of the energy barrier separating the two states, it is interesting to remark that some crystallographic results have been interpreted as containing B_{II} phosphates when in fact these conformations correspond to $\epsilon-\zeta$ values of roughly +30° (see, for example, 10) which in the light of our findings should be considered B_I.

The barrier heights and transition energies are given in the upper part of table 1. From this data it can be seen that the central

CpG dinucleotide can transit very easily to the B_{II} state, losing less than 2 Kcal/mol after crossing a barrier of less than 5 Kcal/mol and causing only local structural changes (see below). The other two junctions yield less stable B_{II} conformations and also have higher transition barriers. Surprisingly, the coupled transition of T3pG4 and C9pA10 leads to the most stable state, but this requires passing a very high energy barrier of 15 Kcal/mol and, as we will see shortly, leads to major structural changes.

The remaining junctions we have studied (G4pC5, A5pC6, G7pT8, T8pC9) do not resonate at low field and thus would not be expected to be in the B_{II} state. However, from the transitions shown graphically in figure 3 (right hand side) and the energies given in the lower half of table 1, we can see that these transitions are not notably more difficult than those of the junctions already discussed. It is also interesting to note that in the case of A5pC6 and T8pC9 junctions, the transition to B_{II} almost causes the facing phosphate to change at the same time with final $\epsilon-\zeta$ values of $+18°$ and $+26°$ respectively.

Analyzing the energy components of the transition energy, it is found in passing from the B_I to the B_{II} state, roughly 0.5−1.5 Kcal/mol of stacking energy is lost at junctions where only one strand is in the B_{II} state, whereas 5−9 Kcal/mol are lost when both phosphates transit. This effect has also been observed and discussed in terms of base overlap in interpreting the effects of B_{II} junctions in crystals (10,25).

It is also found that, for the junctions whose phosphates do not resonate at low field, the torsional energy of the B_{II} conformation is uniformly less stable than that of the starting structure. Despite this finding, the two classes of junction we have created on the basis of their phosphorus chemical shift cannot be clearly distinguished in terms of the energetics of the B_I-B_{II} transition. However, as we will see in section (iii), the structural impact of the transition within each class is very different.

Comparison with NMR data for the CRE dodecamer

We first question we would like to answer is whether any of the B_{II} junctions created above are actually present in the solution structure of CATGACGTCATG or whether they could play a significant role in an equilibrium of different solution conformations. To answer this query we have compared the available NMR data (14) with the values derived from the model conformations before and after the B_I-B_{II} transition. The results in figure 4 involve the junctions whose phosphates resonate to low field and figure 5 shows the remaining junctions investigated. In each case only those parameters changing significantly during the transition are shown. Although figures 4 and 5 only indicate parameter values corresponding to the B_I and B_{II} energy minima the changes occurring during the transition are found to be smooth and monotonic.

For the first class of junctions shown in figure 4, the structural changes are localized at the step and in the strand where the B_I-B_{II} transition takes place. The only exception to this rule occurs for the combined transition of the steps T3pG4 and C9pA10 where changes are also seen to occur in the centre of the dodecamer. However, the most important point to note is that the B_{II} conformations lead to a poorer correlation with the NMR data in all cases. It thus seems that B_{II} conformations do not occur for these steps. Moreover since the structural changes associated with the transition occur monotonically, it seems that a significant B_{II} contribution to a conformational equilibrium can

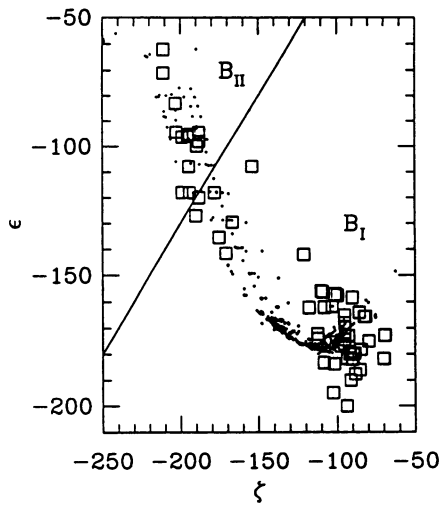

Figure 9. Correlation between ϵ and ζ. Dots correspond to model conformations and squares to crystallographic results. The diagonal line $\epsilon-\zeta=70°$ corresponds to the separation between B_{II} conformations and intermediate or B_I conformations.

also be ruled out. It can also be added that if these steps deform towards more negative values of $\epsilon-\zeta$ (around $-100°$ rather than their naturally stable values of roughly $-30°$) the associated inter-proton distances hardly change, however the sugar phases resemble those of the B_{II} state and are therefore once again in disagreement with the NMR data.

For the remaining steps shown in figure 5, structural changes occur in the sugar puckers at and beyond the site of the backbone transition leading to much worse correlation with the NMR data. The inter-proton distances are also in much poorer agreement with the NMR data after the creation of B_{II} sites. The overall correlation coefficient is found to decrease from 0.97 to 0.82, many distances being violated by more than 1Å and a number of important qualitative base-base distances being lost. Neither of these effects are observed with B_I conformations. The only exception to this result involves the G4pA5 site which does not suffer any major perturbation upon the introduction of a B_{II} conformation. However, a B_{II} site at this junction can be ruled out by the very high chemical shift of the associated phosphate.

In this test, we have compared the minimal energy conformations of the dodecamer before and after B_I-B_{II} transitions. It should however be remarked that these optimized B_{II} forms are not compatible with the B_{II} e values deduced from the COSY coupling constants via the modified Karplus curve. These latter values lie close to $-70°$ as shown in table 2 rather than around $-100°$ as found in oligomer crystals and by the modelling we have carried out. We have thus tried to fit to the NMR data by imposing these ϵ values (on one junction at a time) while also constraining the sugar puckers to agree with the COSY data.

The results of this test are that the energy required to reach this state is much higher than that leading to the optimized B_{II} conformations, overall losses varying from 12 to 40 Kcal/mol (with the exception of the C6pG7 junction which nevertheless loses 6 Kcal/mol). In all cases the final structures are unstable and releasing the constraints results in a passage to the previously optimized B_{II} conformations with ϵ around $-100°$. The structures under constraint, in common with the relaxed B_{II}

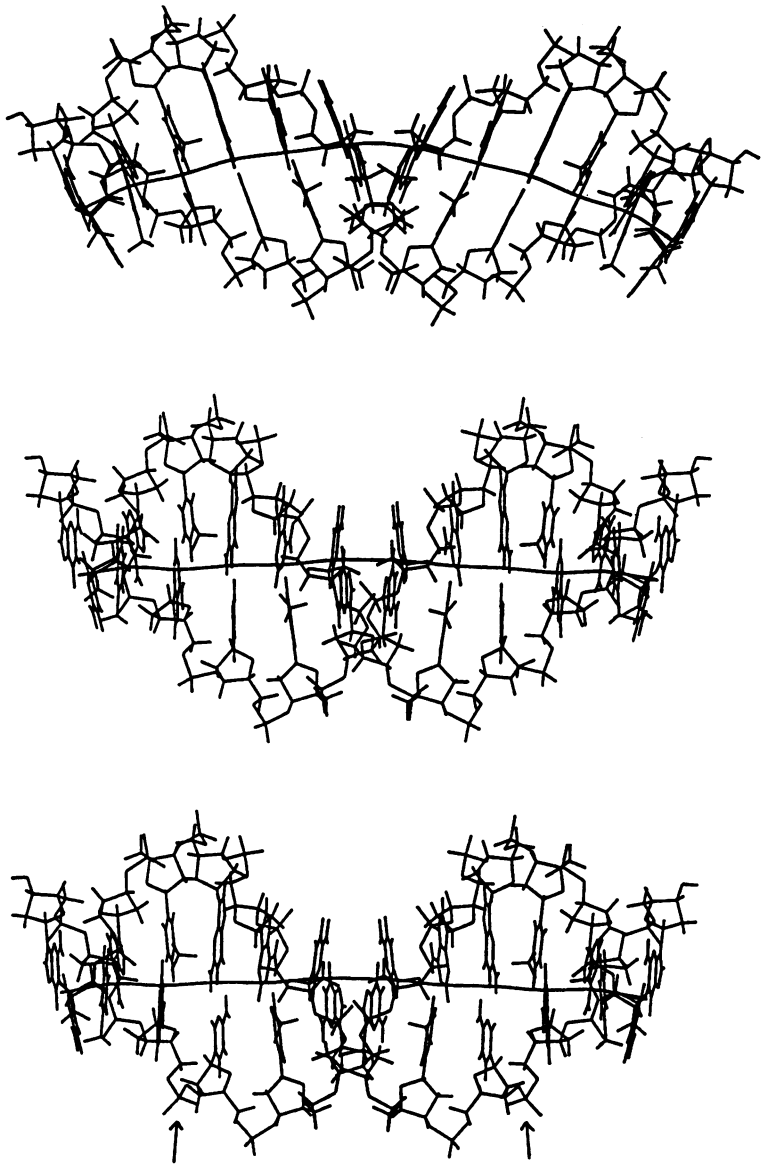

Figure 10. Conformations of the CRE oligomer with and without B_{II} junctions. Centre: optimal conformation with only B_I junctions, Left: a central B_{II} junction in both strands at C6pG7 causing kinking of the duplex, Right: two symmetry related single strand B_{II} junctions at C9pA10 (indicated by arrows). The optimal helical axis is shown in each case.

conformations, also show poor agreement with the NMR interproton distances. Combinations of more than one B_I-B_{II} transition have also been attempted and always led to even greater energy losses. It thus seems possible to conclude that no B_{II} junctions play significant roles in the solution conformation of the CRE dodecamer.

Structural aspects of the B_I-B_{II} transition

We will begin by discussing the role of sugar puckering which we have recently suggested is central to characterising the fine structure of the DNA double helix (17). We have shown that, within the B family of conformations, sugars adopt one of three states (see figure 6): high phase, low amplitude C2′-endo (termed 'S'), low phase, high amplitude C2′-endo (termed 'X') and O1′-endo (termed 'E'). A dinucleotide junction can therefore be described by two letters indicating the two sugar puckers involved (in the conventional 5′ → 3′ direction).

If we consider the B_{II} conformations we have created within the CRE dodecamer in this light, it is found that they all belong to junctions of the type XS or XX. As shown in figure 7, sugar phase and amplitude are clearly correlated and this both for our modelling conformations and for crystallographically resolved oligomers. The three phosphates resonating at low field in the CRE dodecamer already belong to XS junctions in the B_I state. The other junctions are all of the type SX in the B_I state, but are forced to become XS or XX after the imposed transition. During these transitions, both the phase and the amplitude of the sugar at the 5′-side of the junction are closely coupled to the value of $\epsilon-\zeta$.

The fact that B_{II} junctions are synonymous with XS or XX sugar puckers finds support in recent crystallographic data (5,10,24,25). Of the 15 B_{II} junctions observed in these studies all correspond to XS or XX sugar puckers. One can also note that these 15 cases, are pyr-pur (9 cases) or pur-pur (6 cases).

The occurrence of B_{II} junctions in both strands at the same level is also strongly favoured for pyr-pur steps (8 out of 9 cases) compared to pur-pur sequences (2 out of 6 cases, one involving a GA mismatch and the other involving a methylated cytosine). It is interesting to remark that the pur-pyr junctions in the CRE dodecamer have the highest barriers to the B_{II} transition. The pur-pyr G7pT8 junction also led to the creation of a C3′-endo sugar pucker in the nucleotide at the 5′-end of the junction (C6).

The rotation of the phosphate group towards the minor groove following a B_I-B_{II} transition (involving the central CpG junction) is shown in figure 8. One can note that this rotation has little effect on the orientation of the adjacent phosphate. Note that ϵ and ζ respectively are the two dihedrals lying below the phosphate groups. The relationship between ϵ and ζ is shown in figure 9. This correlation is roughly linear for ζ values below $-150°$, but quadratic for less negative values. The crystallographic results show a good correlation which the modelling results, both for the extreme B_I and B_{II} states and for the intermediate transition region, although there is a bigger scatter of ϵ values in the B_{II} zone than the modelling would suggest.

Lastly, we consider the helicoidal parameter changes occurring after B_I-B_{II} transitions. When the final conformation results in a B_{II} junction facing a B_I junction in the other strand, little change is seen in the helicoidal parameters (figure 10). The only significant modifications involve shift and slide which increase slightly (by up to roughly 0.4Å). On the other hand, when two B_{II} junctions face one another large changes are seen (figure 10). In these cases, shift increases by up to 1Å and Xdisp also increases sharply. It is worth stressing that both modelling and experimental results show that Xdisp can become strongly positive in these cases (up to +2Å) indicating that the rotation of the phosphate groups towards the minor groove pushes the base pairs away and into the major groove. To avoid losses in global stacking energy, this movement can occur even far from the B_{II} junctions, causing more positive Xdisp values throughout an oligomer. Rise is also found to increase (by up to 0.8Å) and roll becomes strongly negative (up to $-35°$) inducing a local kink of the double helix towards the minor groove (figure 11). Analyzing the crystallographic oligomers which exhibit B_{II} junctions also shows the presence of negative roll, however no overall curvature is seen since the neighbouring steps adopt positive rolls (5). This observation has been interpreted as crystal packing effect, which would seem to agree with our observations.

In the case of junctions which were not initially XS, we also observe an increase in twist (figure 11), in agreement with the correlations already noted in our previous studies of B-DNA (17). Since XS junctions already have high twist before transition, all our calculations show B_{II} states to be associated with high twist. This is in agreement with both crystallographic data and recent NMR studies where a B_{II} junction is found to occur at a base pair mismatch site (9).

CONCLUSIONS

This modelling study leads to the conclusion that B_{II} conformations are incompatible with the solution structure of the CRE dodecamer. Junctions whose sugar puckers can be classified as XS can be transformed to the B_{II} state with less structural perturbation and, in particular, little effect on the facing strand, but this does not imply that the energetics of the transition is easier in these cases. Junctions which are initially SX create more

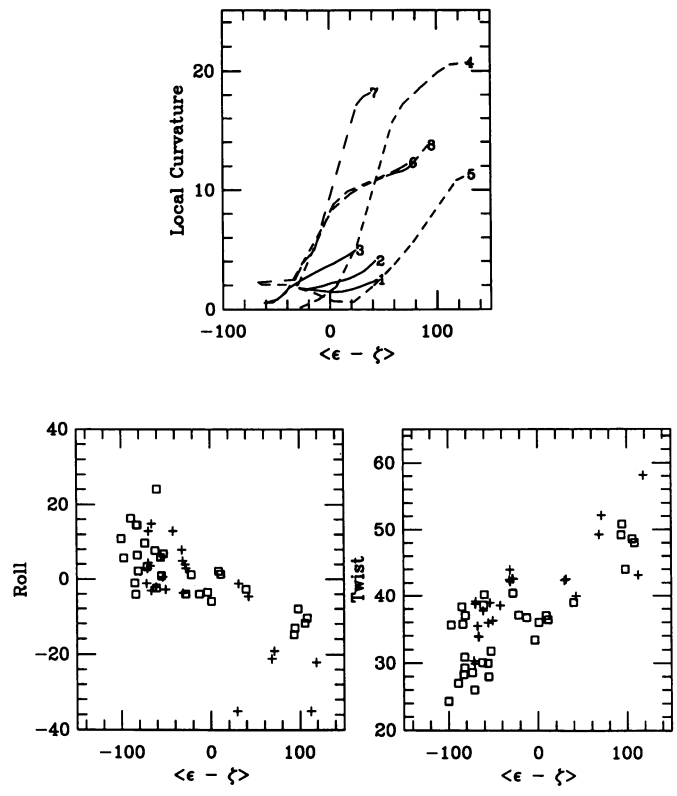

Figure 11. Structural deformations linked to the B_I-B_{II} transitions. The upper diagram shows the evolution of local curvature (angle between successive helical axis vectors in degrees) as B_{II} sites are created (numbers indicate the junctions involved, see caption to figure 3). The lower diagrams show roll and twist as a function of $\epsilon-\zeta$ for minimal energy model conformations (crosses) and for crystallographic results (squares).

disturbance, are transformed to either XS or XX puckers and push the facing junction in the direction of smaller $\epsilon-\zeta$ values (between 26° and $-12°$). It should be noted that these conformational properties of B_{II} junctions are confirmed by crystallographic data, even for oligomers containing other perturbations such as mismatches or methylation, and, also, independently of any possible crystal packing effects. It should also be noted that this study confirms our earlier remarks concerning the importance of the backbone conformations in determining the helical structure of DNA and, notably, twist angles. This opinion has recently been supported by results of NMR refinements taking specifically into account data on backbone dihedral angles (29).

The CpG within the central tetramer (ACGT) of the dodecamer studied appears to be a special case. Although its passage from B_I to B_{II} represents a small loss in energy, the barrier to the transition is very low. Once the B_{II} state is generated local structural perturbations lead to a kink towards the minor groove.

Other modelling studies using molecular dynamics to investigate DNA oligomers have also observed rapid, but infrequent, B_I-B_{II} transitions (30–32). In two different studies, which both simulated DNA surrounded by water and counterions, a single transition occurred during respectively 60ps and 140ps. In the former study the transition occurred within a homopolymeric AT sequence, while in the second a GpA junction (of type XS) was concerned.

ACKNOWLEDGEMENT

The authors thank the Association for International Cancer Research (St. Andrews University, UK) for their generous support of this project.

REFERENCES

1. Privé, G.G., Heinemann, U., Chandrasekharan, S. Kan, L.S., Kopta, M.L. and Dickerson, R.E. (1987) Science, 238, 498–504.
2. Gupta, G. Bansal, M. and Sasisekharan, V. (1980) Proc. Natl. Acad. Sci. USA, 77, 6486–6490.
3. Dickerson, R.E., Goodsell, D.S., Kopta M.L. and Pjura, P.E. (1987) J. Biomol. Struct. Dyn., 5,557–579.
4. Jain, S. and Sundaralingam, M. (1989) J. Biol. Chem., 264, 12780–12784.
5. Heinemann, U. and Hahn, M. (1992) J. Biol. Chem., 267, 7332–7341.
6. Sklenar, V., and Bax, A. (1987) J. Am. Chem. Soc., 109, 7525–7526.
7. Nikonowicz, E.P., and Gorenstein, D.G. (1990) Biochemistry, 29, 8845–8858.
8. Roongta, V.A., Jones, R. and Gorenstein, D.G. (1990) Biochemistry, 29, 5245–5258.
9. Chou, S.H., Cheng, J.W., Fedoroff, O.Y., Chuprina, V.P. and Reid, B.R. (1992) J. Am. Chem. Soc., 114, 3114–3115
10. Privé, G.G., Yanagi, K. and Dickerson, R.E. (1991) J. Mol. Biol. 217, 177–199.
11. Lavery, R. (1988). in 'Structure and Expression Vol.3 DNA Bending and Curvature' (Olson, W. K., Sarma, R. H., Sarma, M. H. and Sundaralingam, M. eds). Adenine Press p191–211.
12. Montminy, M.R., Sevarino, K.A., Wagner, J.A., Mandel, G., Goodman, R.H. (1988) Proc. Natl. Acad. Sci. (USA), 83, 6682–6686.
13. Ziff, E.B. (1990) Trends in Genetics, 6, 69–72.
14. Mauffret, O., Hartmann, B., Convert, O., Lavery, R. and Fermandjian, S. (1992) J. Mol. Biol., in press.
15. Ramstein, J. and Lavery, R. (1988) Proc. Natl. Acad. Sci. (USA), 85, 7231–7235.
16. Hartmann, B., Malfoy, B. and Lavery, R. (1989) J. Mol. Biol., 207, 433–444.
17. Poncin, M., Hartmann, B. and Lavery, R. (1992) J. Mol. Biol., in press.
18. Sun, J.S., Mergny, J.L., Lavery R., Montenay-Garestier, T. and Hélène, C. (1991) J. Biomol. Struct. Dyn., 9, 411–424.
19. Zakrzewska, K. (1992) J. Biomol. Struct. Dynam., 9, 681–695.
20. Lavery, R., Zakrzewska, K. and Pullman, A. (1984) J. Comp. Chem., 5, 363–373.
21. Lavery, R., Sklenar, H., Zakrzewska, K. and Pullman, B. (1986a) J. Biomol. Struct. Dynam., 3, 989–1014.
22. Lavery, R., Parker, I. and Kendrick, J. (1986b) J. Biomol. Struct. Dynam., 4, 443–461.
23. Hingerty, B., Richie, R.H., Ferrel, T.L. and Turner, J.E. (1985) Biopolymers, 24, 427–439.
24. Heinemann, U. and Alings, C. (1989) J. Mol. Biol., 210, 369–381.
25. Grzeskowiak, K., Yanagi, K., Privé, G.G. and Dickerson, R.E. (1991) J. Biol. Chem., 266, 8861–8883
26. Lavery, R. and Sklenar, H. (1988). J. Biomol. Struct. Dynam., 6, 63–91.
27. Lavery, R. and Sklenar, H. (1989). J. Biomol. Struct. Dynam., 6, 655–667.
28. Dickerson, R.E., Bansal, M., Calladine, C.R., Diekmann, S., Hunter, W.N., Kennard, O., Lavery, R., Nelson, H.C.M., Olson, W.K., Saenger, W., Shakked, Z., Sklenar, H., Soumpasis, D.M., Tung, C.-S., von Kitzing, E., Wang, A.H.-J. and Zhurkin, V.B. (1989) J. Mol. Biol., 205, 787–791.
29. Kim, S.G., Lin, L.J. and Reid, B.R. (1992) Biochemistry, 31, 3564–3574.
30. Withka J.M., Swaminathan, S., Beveridge, D.L. and Bolton, P.H. (1991) J. Am. Chem. Soc., 113, 5041–5049.
31. Swaminathan, S., Ravishanker, G. and Beveridge, D.L. (1991) J. Am. Chem. Soc., 113, 5027–5040.
32. Brahms, S., Fritsch, V., Brahms, J.G. and Westhof, E. (1992) J. Mol. Biol. 223, 455–476.